Spatial Localization of Electromagnetic Radiation Sources by Cascade Neural Network Model with Noise Reduction

Milan ILIC [1], Zoran STANKOVIC [2], Natasa MALES ILIC [2]

[1] Inst. of Networked and Embedded Systems, Alpen-Adria-University Klagenfurt, Universitätsstraße 65/67, 9020 Klagenfurt, Austria
[2] Dept. of Telecommunication, University of Nis, Faculty of Electronic Engineering, Aleksandra Medvedeva 14, 18000 Nis, Serbia

ilic@lakeside-labs.at, {zoran.stankovic, natasa.males.ilic}@elfak.ni.ac.rs

Submitted February 28, 2023 / Accepted June 21, 2023 / Online first July 31, 2023

Abstract. *In this paper, the Direction of Arrival - DoA estimation for two mobile sources was performed by using the Single Multilayer Perceptron (MLP) neural network model (SMLP-DoA) and the Cascade MLP model(CMLP). The latter model consists of two neural networks connected in a cascade where the outputs of the first MLP that rejects noise represent the inputs to the second network in a cascade. The outputs of the neural network models determine the direction of arrival of the incoming signals. Two cases were considered, in the first case the neural networks were trained on the samples that were without noise, and in the second with samples containing noise. Both considered neural network models were tested with noisy samples. The results of these two neural models are compared to the results achieved by the RootMUSIC algorithm. The presented results show that the proposed CMLP model has a higher accuracy in determining the angular positions of sources compared to the classical SMLP-DoA model and the RootMUSIC algorithm. Moreover, the CMLP model executes significantly faster compared to the model based on the RootMUSIC algorithm.*

Keywords

The Direction of Arrival (DoA) estimation, artificial neural networks, Multilayer Perceptron (MLP), single MLP, cascade MLP, RootMUSIC algorithm

1. Introduction

Estimation of the direction of arrival (DoA) from data collected by sensor arrays is essential for various applications such as radars, sonars, wireless communications, geophysics, biomedical engineering, and others. In the last three decades, there has been significant progress in the development of algorithms that are applied to solving the problem of determining the direction of incoming electromagnetic (EM) signals. With the emergence of new technologies applied in today's 5G systems, which include massive MIMO systems and adaptive beamforming, the application of DoA estimation for obtaining information about the direction of the user's signal in mobile communication systems is especially important. Space signal processing by using an adaptive antenna array is one approach to reducing the impact of interference and noise on the signal and increasing the capacity and speed of the channel in wireless communication systems. The vital parts in the antenna array beamforming are the methods for deriving the position and space localization in 1D and 2D spaces of the incoming wave called the direction of arrival, DoA, estimation. Based on the obtained data, it is possible to direct the radiation characteristics of the antenna array toward a specific user, while minimizing interference from other mobile users [1].

Classical approaches in DoA estimation that are based on the application of superresolution algorithms (MUSIC and its modifications [1–4], ESPRIT [1]) provide results of high accuracy. However, they require a powerful hardware platform and a significant amount of time to complete very complex matrix calculations. These disadvantages in conditions of limited hardware resources make superresolution algorithms quite unsuitable for real-time applications. An alternative approach in DoA estimation based on the application of artificial neural networks, ANN, [5–7] can enable the creation of DoA neural models whose accuracy is in the range of accuracy of superresolution algorithms. In addition, the calculation speed of these models is much higher than by using the superresolution algorithms since ANN-based models do not require a powerful hardware platform for performing complex matrix calculations. These facts can be approved by the papers that apply the ANN in DoA estimation in wireless communications [8–15], and papers relating to the application of ANN in DoA estimation in acoustics such as the analysis and results given in [16]. It is shown that in conditions of increased noise power, the accuracy of DoA neural models

DOI: 10.13164/re.2023.0381

can significantly decrease [10], [11]. Accordingly, the main idea of this paper is to develop an ANN model that will be more accurate for DoA estimation in high noise power conditions. The neural network-based models used in this paper for DoA estimation are the Single MLP (Multi-Layer Perceptron) model (SMLP-DoA) and the two-stage cascade MLP model (CMLP). The first stage in the CMLP model is formed to reduce the noise in the spatial correlation matrix, while the second stage should determine the DoA angles. Since the second stage receives a matrix that is largely cleaned of noise, it will be able to determine DoA angles with better punctuality than neural models that perform DoA estimation directly over the noisy matrix.

The paper is organized as follows: After the Introduction, in Sec. 2 and Sec. 3, the architecture of the models is described. Section 4 relates to the application scenarios of two neural network models. The results obtained by applying these models to specific examples for two users are presented, under different scenarios, which include noiseless and noisy conditions for different values of the signal-to-noise ratio (*SNR*) and the number of samples for training the network. The achieved results are compared to the results obtained by the RootMUSIC algorithm. In this paper, the simulation of neural models is performed in a real environment when uncorrelated White Gaussian noise is present on the antenna array. Comparison of the accuracy of the developed SMLP-DoA and CMLP neural models with the RootMUSIC algorithm is performed by analyzing the root mean square error (*RMSE*) and the root mean value of Cramer-Rao Lower Bound (*rmCRLB*) that those models expressed on the test samples. Moreover, the time required for DoA estimation using the mentioned neural models and the RootMUSIC algorithm is compared. In Sec. 5, the Conclusion is given and after that an overview of the used literature.

2. Single MLP-DoA Model

The single MLP-DoA model consists of an MLP neural network and its architecture is shown in Fig. 1.

For the development of neural models, the first row of the spatial correlation matrix, without the R_{11} element, is used as given by (1), which is normalized by the power p_{rin} and is shown by (2).

$$\tilde{\mathbf{p}} = \left[\widetilde{p_i}\right]_{1x(N-1)}, \widetilde{p_i} = R^{(\text{n})}_{1(i+1)},\ i = 1,2,\ldots,N-1, \quad (1)$$

$$\mathbf{p} = \left[\frac{\widetilde{p_1}}{p_{\text{rin}}}\ \frac{\widetilde{p_2}}{p_{\text{rin}}}\ \ldots\ \frac{\widetilde{p_i}}{p_{\text{rin}}}\ldots\frac{\widetilde{p_{N-1}}}{p_{\text{rin}}}\right] = \frac{\tilde{\mathbf{p}}}{p_{\text{rin}}}. \quad (2)$$

By excluding the R_{11} element (autocorrelation element) from the training of the neural model, the influence of noise present on the main diagonal of the correlation matrix is removed. The goal of forming the normalized vector $\mathbf{p}$ is the invariance of its elements when changing the distance of the signal source r as well as its power p_{rin}.

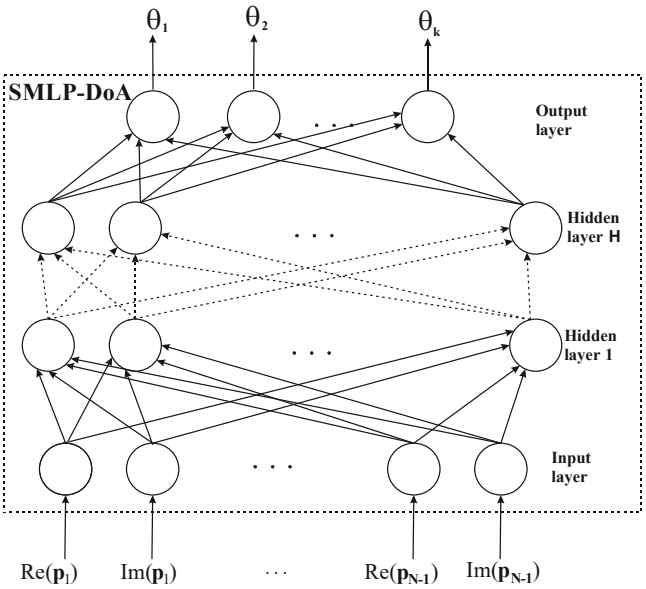

Fig. 1. Architecture of the SMLP-DoA neural network for 1D DoA estimation.

The task of the SMLP model is to extract information about the position of the user in the signal space, which is contained in the elements of the first row of the spatial correlation matrix without the first element, and to determine the position of the user in the 1D DoA space using this information. The vector of azimuth coordinates of K user sources is represented by the following expression:

$$\left[\theta_1\theta_2\ldots\theta_s\ldots\theta_K\right]^{\text{T}} = f_{\text{SMLP-DoA}}\left(\mathbf{p}\right) \quad (3)$$

where $f_{\text{SMLP-DoA}}(\cdot)$ represents the transfer function of the MLP model. The transfer function of the MLP model is described by the transfer function of the MLP neuron [10], [11] as:

$$\mathbf{y}_i = F\left(\mathbf{w}_i\mathbf{y}_{i-1} + \mathbf{b}_i\right), \quad i = 1,2,\ldots,H \quad (4)$$

where $\mathbf{y}_{i-1}$ vector represents the output of the $(i-1)$ hidden layer, $\mathbf{w}_i$ represents the matrix of connection weights between neurons of the $(i-1)^{\text{th}}$ hidden layer and neurons of the i^{th} hidden layer, $\mathbf{b}_i$ is a vector containing the thresholds of the i^{th} hidden layer and H represents the number of hidden layers. The transfer function of the neurons in the hidden layers F is the hyperbolic tangent sigmoidal function [7]:

$$F\left(u\right) = \frac{\text{e}^{u} - \text{e}^{-u}}{\text{e}^{u} + \text{e}^{-u}}. \quad (5)$$

The real and imaginary parts of the spatial correlation matrix are fed separately to the input of the MLP neural network. Otherwise, bringing complex quantities to the input of the MLP network complicates the architecture and implementation of the network model as well as its training. The input layer of the neural network is:

$$\mathbf{y}_0 = \left[\text{Re}\left\{\mathbf{p}_1\right\}\text{Im}\left\{\mathbf{p}_1\right\}\text{Re}\left\{\mathbf{p}_2\right\}\text{Im}\left\{\mathbf{p}_2\right\}\ldots \text{Re}\left\{\mathbf{p}_{N-1}\right\}\text{Im}\left\{\mathbf{p}_{N-1}\right\}\right]_{1\times 2(N-1)}. \quad (6)$$

The output of the neural network is represented by the following expression, [11]:

$$\left[\theta_1\theta_2 \ldots \theta_s \ldots \theta_K\right]^{\mathrm{T}} = \mathbf{w}_{H+1}\mathbf{y}_H \tag{7}$$

where $\mathbf{w}_{H+1}$ represents the matrix of connection weights between neurons in the last hidden layer and neurons in the output layer. During the neural network training process, the weight matrices $\mathbf{w}_1, \mathbf{w}_2, \ldots, \mathbf{w}_H, \mathbf{w}_{H+1}$, and threshold values are optimized to achieve satisfactory mapping accuracy. The notation used to define the MLP neural network is MLPN_{l}-N_i-N_H where N_{l} is the total number of layers, H is the total number of hidden layers, and N_i is the total number of neurons in the i^{th} hidden layer.

3. Cascade MLP Neural Model (CMLP)

The cascade model, shown in Fig. 2, is composed of two MLP neural models that are connected in a cascade where the outputs of the first model represent the inputs of the second one.

The first model in the cascade is the Noise Reduction MLP neural network (MLP-NR), which has the task of reducing the presence of noise in the elements of the first row of the correlation matrix without the first element. The second model in the cascade consisting of an MLP neural network (MLP-DoA) should determine the user's azimuth position in 1D DoA space. The architecture of the MLP-DoA network is the same as the architecture of the SMLP-DoA neural network. The vector of azimuth coordinates of K user sources is given by the expression:

$$\begin{aligned}\left[\theta_1\theta_2 \ldots \theta_s \ldots \theta_K\right]^{\mathrm{T}} &= f_{\mathrm{CMLP}}\left(\mathbf{p}\right) = \\ f_{\mathrm{MLP\text{-}DoA}}\left(f_{\mathrm{MLP\text{-}NR}}\left(\mathbf{p}\right)\right) &= f_{\mathrm{MLP\text{-}DoA}}\left(\bar{\mathbf{p}}\right)\end{aligned} \tag{8}$$

where $f_{\mathrm{CMLP}}(\cdot)$ represents the transfer function of the cascade model, CMLP. The transfer functions of the MLP-NR model, $f_{\mathrm{MLP\text{-}NR}}$, and MLP-DoA model, $f_{\mathrm{MLP\text{-}DoA}}$, are described by the transfer function of the MLP neuron as given by (4). Inputs of the MLP-NR in the CMLP model are as given by (6). The outputs of the MLP-NR are fed to the MLP-DoA neural model, whereas the outputs of the MLP-DoA neural network are the same as the outputs of the SMLP-DoA model, as given by (7).

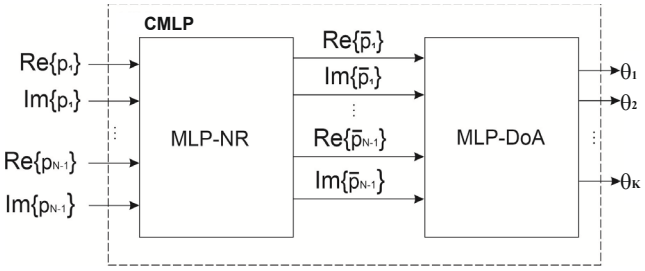

Fig. 2. Architecture of the CMLP neural model for 1D DoA estimation.

4. Training and Testing Data

All models analyzed in the paper, the RootMUSIC and the neural network models (SMLP-DoA and CMLP), were programmed in the MATLAB environment, which was installed on the hardware platform (AMD Phenom™ II X4 965 processor-3.4 GHz, RAM-4 GB).

The parameters generated for the training and testing of two MLP neural network models – the SMLP-DoA and CMLP are listed in Tab. 1. The Levenberg-Marquardt algorithm was used for training the MLP network using MATLAB software. Simulation of two signal sources that can be found in the azimuth position from the range of –30° to 30° (azimuth angle beamwidth of the antenna array) was considered. The antenna array with four elements, which are distanced by half wavelength, was used for sampling the signals emitted from the sources. The values of the signal-to-noise ratio range from –10 dB to 15 dB.

The training and test sets are formed as follows:

$$\left\{\begin{array}{c}\left(\mathbf{p}^{\mathrm{t}}\left(\theta_1^{\mathrm{t}}, \theta_2^{\mathrm{t}}, SNR^{\mathrm{t}}\right), R_{\mathrm{l}(i+1)},\ i = 1, 2, \ldots,\ \mathrm{N}-1\right) \mid \\ \theta_1^{\mathrm{t}} \in \left[-30 : \theta_{\mathrm{step}}^{\mathrm{t}} : 30\right],\ \theta_2^{\mathrm{t}} \in \left[-30 : \theta_{\mathrm{step}}^{\mathrm{t}} : 30\right],\ \theta_1^{\mathrm{t}} > \theta_2^{\mathrm{t}}, \\ SNR^{\mathrm{t}} \in \left[-10 : SNR_{\mathrm{step}}^{\mathrm{t}} : 15\right]\end{array}\right\} \tag{9}$$

The neural network is trained in the same manner for samples without noise and samples with noise. In the first case, an ideal correlation matrix is used, which is formed on signal samples from the antenna array that do not have noise, so that only the values of the user's position θ^{t}_1 and θ^{t}_2, are used to form the training set. The step value for training the network is $\theta^{\mathrm{t}}_{\mathrm{step}} = 0.5$ for both users and 7 260 samples were generated. The data set for testing the network was formed under the influence of noise.

In the second case, a real correlation matrix is used, which is formed on signal samples from the antenna array, which have noise. The parameter values for the training process in the case of both users are $\theta^{\mathrm{t}}_{\mathrm{step}} = 1$, $SNR^{\mathrm{t}}_{\mathrm{step}} = 1.8$, while the values for the test are $\theta^{\mathrm{t}}_{\mathrm{step}} = 1.3$, $SNR^{\mathrm{t}}_{\mathrm{step}} = 2$. The sample number used for training is 25 620, while 14 053 samples were formed for the test.

Based on our earlier research in the field of application of the classical MLP model in DoA estimation [10], [11], when applying a uniform distribution of network samples, the selected sampling steps provide the required amount of data for training DoA neural models with satisfactory accuracy. This avoids generating a too large train-

Azimuth angle beamwidth of the antenna array	$[\theta_{\min}, \theta_{\max}] = [-30°, 30°]$
Signal source number	$K = 2$
Signal-to-noise ratio range	$[SNR_{\min}, SNR_{\max}] =$ [–10 dB, 15 dB]
Array antenna number	$N = 4$
Array element distance	$d = \lambda/2$

Tab. 1. Parameters used in training and testing neural models for the case of two users.

ing set which will significantly slow down the neural models' training algorithm. Also, the chosen step for test samples is adequate for evaluating the performance of the developed models for estimating DoA in a large number of points of their input-output space.

It should indicate that in the case of the CMLP model, training of the cascaded MLP-NR and MLP-DoA networks is not performed simultaneously, i.e. the weights and biases of the two networks are changed independently.

4.1 SMLP Model Application Results

The first step in the analysis of DoA estimation at one dimension-1D in the azimuth plane was carried out by the Single Multilayer Perceptron neural network model- SMLP for two users. The following metrics were used in the neural network testing process: worst-case error (WCE), average test error (ATE), and Pearson product-moment correlation coefficient (r^{PPM}) [7].

They were considered for *SNR* from –6 dB to 15 dB to estimate the best results of the SMLP network. As can be seen from Tab. 2 to Tab. 4, the values of the neural network model are better than those of RootMUSIC which shows the largest WCE, the ATE within the usable limits, and a small value of the correlation coefficient. The performed analysis indicates that the results of the RootMUSIC model, in the case of high noise and close sources, may deviate significantly in the determination of the source angular position compared to the proposed neural model.

MLP network	**WCE [%]**	**ATE [%]**	r^{PPM}
MLP4-18-14	**21.6303**	**0.7929**	**0.9983**
MLP4-23-23	21.0274	0.8557	0.9977
MLP4-20-10	25.1206	0.8459	0.9976
MLP4-22-22	21.8815	0.9741	0.9966
MLP4-9-7	22.1416	1.028	0.997
MLP4-22-20	22.3558	0.9221	0.9972

Tab 2. Test results for $SNR^t \in [-6 : 15]$, of six SMLP-DoA networks with the best features, trained on noiseless samples.

MLP network	**WCE [%]**	**ATE [%]**	r^{PPM}
MLP4-20-10	**20.4665**	**0.737**	**0.9984**
MLP4-20-12	19.6322	0.925	0.9976
MLP4-16-11	22.3673	0.9032	0.9976
MLP4-18-7	23.0322	0.9058	0.9977
MLP4-10-10	21.4057	0.9426	0.9974
MLP4-18-16	22.5696	0.9807	0.9969

Tab. 3. Test results for $SNR^t \in [-6 : 15]$, of six SMLP-DoA networks with the best features, trained on noisy samples.

DoA model	**WCE [%]**	**ATE [%]**	r^{PPM}
RootMUSIC	199.3053	4.6599	0.7415

Tab. 4. Test results of RootMUSIC algorithm for $SNR^t \in [-6 : 15]$.

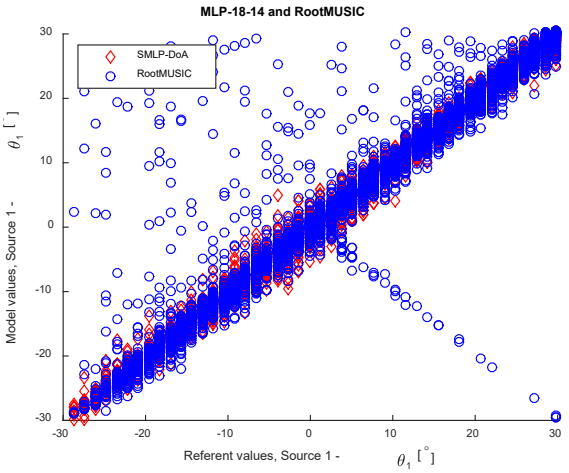

Fig. 3. Scatterplot of the SMLP-DoA model on the test set for $SNR^t \in [-6 : 15]$ when the model was trained on noiseless samples, a) θ_1 output, b) θ_2 output.

The best neural model selected in the case of training on samples without noise is MLP4-18-14, whereas, in the case of training on samples with noise, the neural network MLP4-20-10, which has the highest value of the correlation coefficient and the lowest value of the mean test error, was used for the realization.

The results of DoA estimation in noiseless and noisy networks for the first and second sources are shown as the scatterplot in Fig. 3 and Fig. 4 respectively, along with the results provided by RootMUSIC. It can be seen that, for this range of *SNR*, the SMLP-DoA model gives satisfactory results, while RootMUSIC makes large errors.

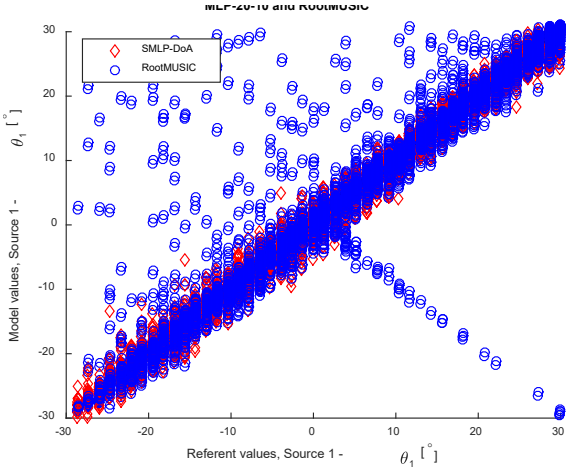

a)

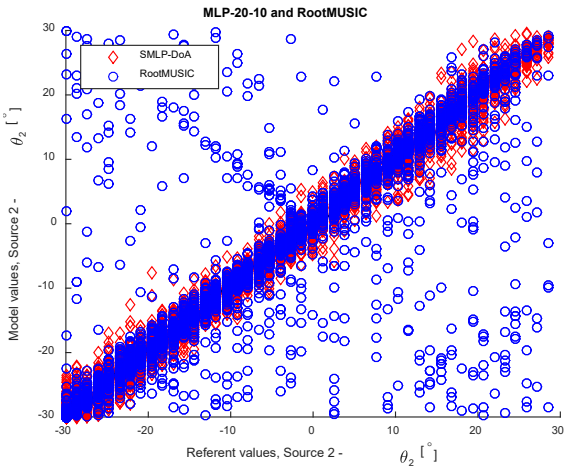

b)

Fig. 4. Scatterplot of the SMLP-DoA model on the test set for $SNR^t \in [-6 : 15]$ when the model was trained on noisy samples, a) θ_1 output, b) θ_2 output.

4.2 CMLP Model Application Results

The cascade model was developed to obtain better DoA estimation results compared to the previously developed SMLP model. It consists of two cascaded MLP models where the first model should reduce the influence of noise appearing on the elements of the correlation matrix. For the training of the first MLP network (MLP-NR), six elements of an ideal correlation matrix that does not contain noise are used. In this way, inputs that include noise should be brought closer to values that do not contain noise and thereby refine the first row of the correlation matrix without the autocorrelation element. The elements of the correlation matrix purified in this procedure are put into the next MLP model in the cascade, which determines the position of the user in the 1D azimuth plane. The name of the second model in the cascade is MLP-DoA and it was trained by both noiseless and noisy samples. The training set of 7 260 samples for the case without noise, and 25 620 training and 14 053 testing samples for the case with noise were formed in the same manner as for the SMLP-DoA model.

MLP network	WCE [%]	ATE [%]	r^{PPM}
MLP4-23-23	**29.7866**	**1.1074**	**0.9964**
MLP4-22-22	30.4	1.0793	0.9964
MLP4-23-23	28.25	1.0974	0.9963
MLP4-22-20	28.5278	1.1087	0.9963
MLP4-22-20	29.0264	1.1269	0.9961
MLP4-23-23	30.7966	1.1342	0.9962

Tab. 5. Test results of six MLP-NR networks with the best characteristics.

MLP network	WCE [%]	ATE [%]	r^{PPM}
MLP4-23-23	**8.3219**	**0.6559**	**0.9993**
MLP4-13-13	7.8419	0.8085	0.999
MLP4-22-20	8.5658	0.7636	0.999
MLP4-16-4	8.672	0.9561	0.9987
MLP4-22-20	8.7465	0.7078	0.9992
MLP4-18-14	9.0153	0.8007	0.9991

Tab. 6. Test results for $SNR^t \in [-6 : 15]$ of six MLP-DoA networks with the best features, trained on noiseless samples.

MLP network	WCE [%]	ATE [%]	r^{PPM}
MLP4-20-10	**8.0734**	**0.7211**	**0.9991**
MLP4-18-16	8.1875	0.7326	0.9992
MLP4-20-10	9.0931	0.6796	0.9992
MLP4-23-23	9.1663	0.689	0.9992
MLP4-16-11	9.174	0.7096	0.9992
MLP4-14-14	9.9398	0.7131	0.9992

Tab. 7. Test results for $SNR^t \in [-6 : 15]$ of six MLP-DoA networks with the best features, trained on noisy samples.

The statistical results of the six best MLP-NR models are shown in Tab. 5. The MLP-NR model selected for further simulation is MLP4-23-23, which has the best ratio of worst-case error, average test error, and correlation coefficient compared to other models. Then, the purified values from the noise are passed through the second MLP-DoA model in cascade, which has the task of determining the users' positions in the azimuth plane. Tables 6 and 7 show the test values for *SNR* range –6 dB to 15 dB for the case of training the MLP-DoA model with samples without noise and for the case of training with noisy samples, respectively. Compared to Tab. 4 which includes the characteristics of the RootMUSIC algorithm, significantly better results for the MLP-DoA models can be seen.

The MLP4-23-23 neural network trained with noiseless samples and the MLP4-20-10 neural network trained on noisy samples were selected for the implementation of the CMLP neural model for DoA estimation since they have the highest r^{PPM} and the lowest ATE.

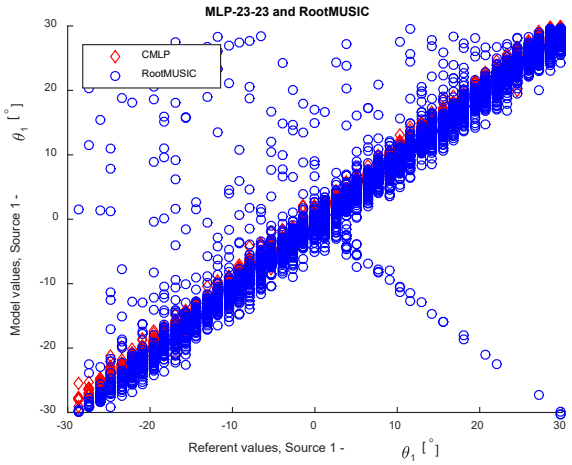

a)

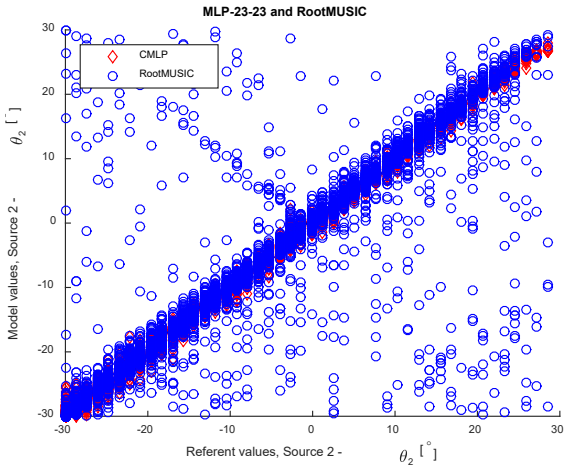

b)

Fig. 5. Scatterplot of the CMLP model on the test set for $SNR^{\mathrm{t}} \in [-6 : 15]$ when the model was trained on noiseless samples, a) θ_1 output, b) θ_2 output.

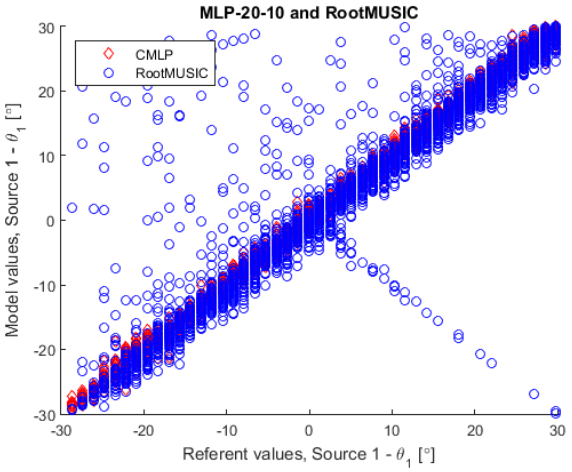

a)

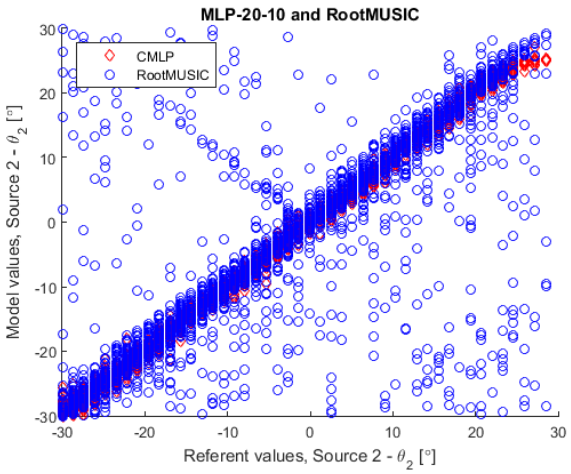

b)

Fig. 6. Scatterplot of the CMLP model on the test set for $SNR^{\mathrm{t}} \in [-6 : 15]$ when the model was trained on noisy samples, a) θ_1 output, b) θ_2 output.

The outputs of the CMLP model trained without and with noise are shown in Fig. 5 and Fig. 6, respectively where the results for the first source are presented under a), and for the second source under b), together with the results provided by RootMUSIC. It can be seen that the CMLP model achieves more accurate results in determining the angular position of the users than the SMLP-DoA model by refinement of the correlation matrix with noise. It can be noticed that the model trained on samples without noise offers better results than the model trained on samples with noise and RootMUSIC algorithm for the observed parameter values.

4.3 Simulation of SMLP-DoA and CMLP Model Application in the Real Scenario

In this part of the paper, the SMLP-DoA and CMLP neural models were applied in the system architecture shown in Fig. 7 which simulates a real environment where two useful signals are present. The MATLAB software was used to estimate the time needed for the execution of the system when the already developed SMLP-DoA or CMLP neural model was implemented within the DoA module and to compare these times with super-resolution RootMUSIC algorithms. It is necessary to determine the distance between the N elements of the antenna array (N has to be greater than the number of sources K), on the bases of the selected receiver sampling frequency f, i.e. $d = \lambda/2 = c/(2f)$. To generate a certain number of snapshots of the signal from the antenna array in a short time interval (N_{s} - number of snapshots) and to create the appropriate form of that signal for further processing the usage of a fast A/D converter and FPGA module is suggested. As mentioned earlier, the neural DoA model utilizes only the correlation matrix without the first element:

$$\tilde{p}_i = R^{(\mathrm{n})}_{1(i+1)} = \frac{1}{N_{\mathrm{s}}} \sum_{s=1}^{N_{\mathrm{s}}} x_1^{(s)} x_{i+1}^{(s)^*}, \quad i = 1, 2, \ldots, N-1 \qquad (10)$$

where $x_i^{(s)}$ is the complex value of the signal at the output of the i^{th} antenna sensor where the s^{th} snapshot was taken. The values of the first row of the correlation matrix calculated in this way were divided by the reference value of power p_{rin} according to (2). Consequently, a normalized sample **p,** independent of the input reference power p_{rin}, is obtained from the signal space and is transferred to the input of the neural DoA model. The neural DoA model, depending on the input pattern **p**, determines the angular position of the signal source.

To simulate signal reception on the antenna array in the conditions in which uncorrelated White Gaussian noise of power σ_n^2 is present on the antenna array, the MATLAB function *wgn* was used. The output of the antenna array *x*, which includes noise, was formed by adding the noise vector obtained at the output of the antenna array by the function *wgn* to the output of the antenna array that originates from the clean signal. The accuracy of the neural model was calculated for different values of *SNR*.

The neural model exactness was evaluated using the root mean square error (*RMSE*) on the outputs of the neural model tested with the noisy test set. The *RMSE* value of the s^{th} output of the model on the test set is defined as follows [7], [11]:

$$RMSE_k = \sqrt{\frac{1}{N_T}\sum_{i=1}^{N_T}\left(\theta_k^{(i)} - \tilde{\theta}_k^{(i)}\right)^2}, \quad k = 1, 2, \ldots, K \quad (11)$$

where $\theta_k^{(i)}$ represents the k^{th} output of the neural model when the value of the i^{th} sample is at the input of the model, $\tilde{\theta}_k^{(i)}$ represents the exact value of the angular position of the k^{th} signal source for the i^{th} sample, and N_T is the number of test samples.

Simulation parameters for two mobile users are given in Tab. 8.

Samples containing noise were fed to the input of the model during the simulation in the form $\{\mathbf{p}^t(\theta^t_1, \theta^t_2, SNR), \theta^t_1, \theta^t_2)\}$ and were taken from the test set generated as follows:

$$\left\{\begin{array}{c} \theta_1^t \in [-30:1.3:30], \\ \theta_2^t \in [-30:1.3:30], \ \theta_1^t > \theta_2^t, \\ SNR \in [-10:2:15] \end{array}\right\}. \quad (12)$$

The test set of 1 081 samples per one *SNR* value from the set of values {–10 dB, –6 dB, –2 dB, 0 dB, 2 dB, 6 dB, 10 dB, 14 dB} was used. The SMLP-DoA and CMLP models trained on noiseless samples, as well as the RootMUSIC algorithm, are observed and compared in Tab. 9 and Fig. 8.

After observing the trained models on samples without noise, the SMLP-DoA and CMLP models trained on samples with noise are analyzed and are also compared with the RootMUSIC algorithm (Tab. 10 and Fig. 9).

The presented results for two users indicate that the application of neural models achieves a much smaller error compared to the error of the RootMUSIC algorithm for both cases of training the network on samples with and without noise, as well as that the error achieved by the CMLP model is the smallest, which is especially pronounced for the *SNR* in range –10 dB to 0 dB.

Additionally, with the aim of a more complete analysis of the performance of the mentioned models, the dependence of the root mean value of *CRLB* (Cramer-Rao

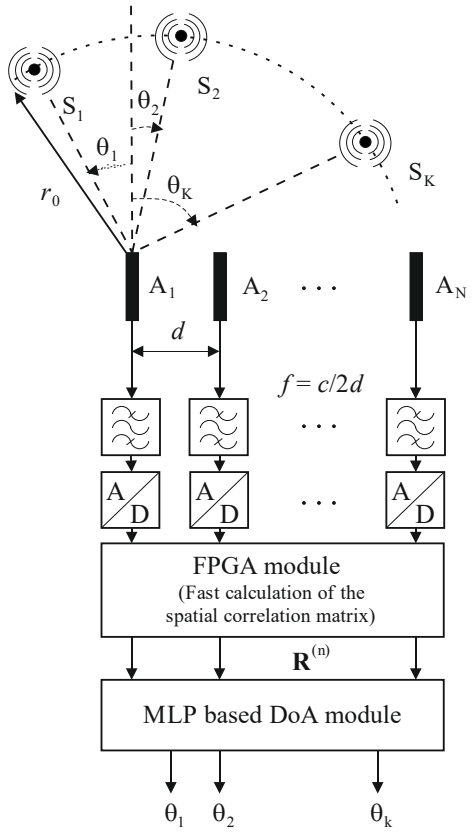

Fig. 7. System architecture for spatial localization of electromagnetic radiation sources based on the antenna array, FPGA module used for spatial correlation matrix calculation, and DoA estimation module.

Azimuth angle beamwidth of the antenna array	$[\theta_{min}, \theta_{max}] = [-30°, 30°]$
Signal source number	$K = 2$
Array antenna number	$N = 4$
Array element distance	$d = \lambda/2$
The distance of the user from the antenna array	$r_0 = 100$ m
Referent signal power the sensor of the antenna array	$p_{rin} = 0.00795$ mW (–21 dBm)
Number of signal samples from the antenna array	$N_s = 500$
***SNR* values considered in simulations of all models**	*SNR* ∈ {–10 dB, –6 dB, –2 dB, 0 dB, 2 dB, 6 dB, 10 dB, 14 dB}

Tab. 8. Simulation parameters in the case of two mobile users.

Model	Model computation time for 1 081 samples	***RMSE* [°]** (Model errors for different signal-to-noise ratios)								
		SNR	–10 dB	–6 dB	–2 dB	0 dB	2 dB	6 dB	10 dB	14 dB
SMLP-DoA	0.0027 s	Source 1	4.57	1.83	0.76	0.51	0.39	0.27	0.26	0.25
		Source 2	5.77	2.32	0.95	0.62	0.43	0.27	0.24	0.24
CMLP	0.0064 s	Source 1	2.86	1.04	0.56	0.47	0.44	0.41	0.42	0.42
		Source 2	2.93	1.09	0.53	0.44	0.41	0.36	0.36	0.36
RootMUSIC	0.64 s	Source 1	14.10	14.15	10.21	8.32	8.81	6.23	4.51	0.76
		Source 2	28.77	22.82	18.02	16.61	13.61	10.99	6.32	0.63
rmCLRB	Source 1, Source2		7.25	4.57	2.89	2.29	1.82	1.15	0.72	0.46

Tab. 9. Comparing the performance of neural models trained on noiseless samples and RootMUSIC for a test set of 14 053 samples for the two-user case.

Model	Model computation time for 1 081 samples	***RMSE* [°]** (Model errors for different signal-to-noise ratios)								
		SNR	–10 dB	–6 dB	–2 dB	0 dB	2 dB	6 dB	10 dB	14 dB
SMLP-DoA	0.0027 s	Source 1	4.45	1.79	0.77	0.51	0.37	0.25	0.24	0.23
		Source 2	5.14	2.09	0.92	0.58	0.39	0.24	0.19	0.18
CMLP	0.0064 s	Source 1	2.81	1.03	0.54	0.44	0.41	0.38	0.38	0.37
		Source 2	2.74	1.08	0.58	0.52	0.49	0.45	0.45	0.45
RootMUSIC	0.64 s	Source 1	14.11	14.16	10.22	8.32	8.82	6.23	4.51	0.76
		Source 2	28.77	22.82	18.02	16.62	13.61	10.99	6.33	0.63
rmCLRB	Source 1, Source2		7.25	4.57	2.89	2.29	1.82	1.15	0.72	0.46

Tab. 10. Comparing the performance of neural models trained on noisy samples and RootMUSIC for a test set of 14 053 samples for the two-user case.

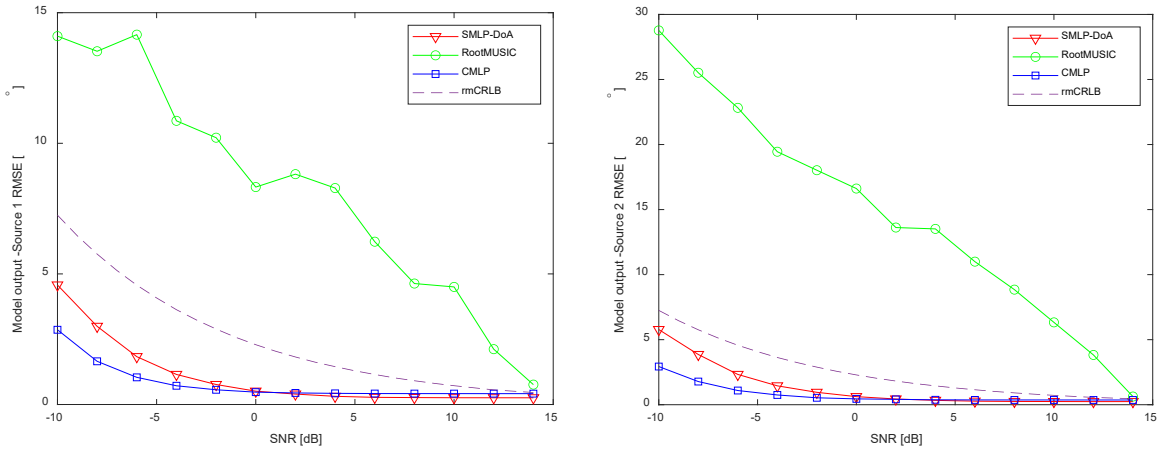

(a) (b)

Fig. 8. Model output errors for different *SNR* values (neural models are trained on noiseless samples) for the case of two users: (a) Output 1, (b) Output 2.

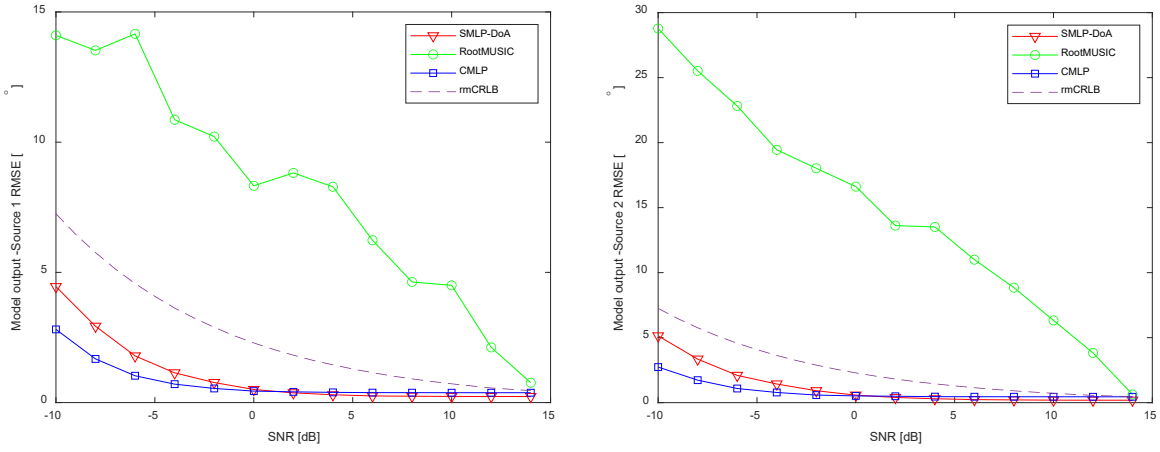

(a) (b)

Fig. 9. Model output errors for different *SNR* values (neural models are trained on noisy samples) for the case of two users: (a) Output 1, (b) Output 2.

Model (Case $K = 2$)	Root MUSIC	SMLP-DoA	CMLP
Time (14 053 samples)	8.36 s	0.036 s	0.083 s
Time per sample	0.595 ms	2.562 μs	5.91 μs

Tab. 11. Time required for DoA estimation of different models.

Lower Bound) [17], [18] of each source on the *SNR* value for the test set, represented by (13), is shown in Tab. 9 and Tab. 10, and Fig. 8 and Fig. 9.

$$rmCRLB_k(SNR) = \sqrt{\frac{1}{N_T}\sum_{i=1}^{N_T} CRLB(\theta_k^{(i)}, SNR)}\ , k = 1,...,K\ . \quad (13)$$

It can be seen that the *RMSE* values of the SMLP-DoA and CMLP models outperform the *rmCRLB* curve. The reason for this is that the proposed neural models show significantly better accuracy in DoA estimation compared to classic unbiased DoA estimator (RootMUSIC) in cases where the signal sources are very close to each other. The results also indicate that the ANN-based DoA estimators are biased, which is hinted in [19].

Table 10 provides a comparison of the time required to process all samples as well as the time required per sample for the case of two users. The results shown in Tab. 11 indicate that the simulation execution time by using artificial neural models is much faster (of the order of 100 times) compared to the time required by the RootMUSIC algorithm. In addition, the SMLP-DoA model executes twice as fast compared to CMLP, which is expected given the more complex architecture of the CMLP model.

The main disadvantage of the RootMUSIC algorithm is that it uses intensive matrix calculations, which in this case where four antennas were used does not represent a serious problem for calculation because the matrices are relatively small. However, if the number of antennas increases to support a larger number of users, RootMUSIC will operate significantly slower due to the processing of a large number of matrix elements.

5. Conclusion

In this paper, the angle of the incoming wave (Direction of Arrival, DoA) was determined by processing the data of the spatial correlation matrix of signals collected by the sensors of the antenna array using the application of artificial neural network models. Two Multilayer Perceptron-MLP neural models were used for DoA estimation, the Single MLP model (SMLP-DoA) and the Cascade MLP model (CMLP). DoA estimation was performed for two users, where the models were trained on samples without the presence of noise or with noise for different values of signal-to-noise ratio, *SNR*. For signal sampling in all scenarios, the antenna array of four elements at a distance of $\lambda/2$ was used, and White Gaussian noise is present. It can be inferred that the RootMUSIC algorithm makes large errors when determining the angular positions of the signal sources in conditions of increased noise (below 0 dB). Accordingly, this algorithm is not usable for the entire range of *SNR* values. Both neural models accomplish better results than the RootMUSIC algorithm. The CMLP model is more accurate than the SMLP-DoA model for all analyzed signal-to-noise ratio values. Moreover, the CMLP model trained on noiseless samples achieves better results than the model trained on samples including noise for the range of the analyzed parameters. Comparing the time required to determine the user angular positions by neural network models and RootMUSIC, it can be concluded that the CMLP model, due to the more complex architecture, has a slightly lower execution time of DoA estimation compared to the SMLP-DoA model. However, this speed is still significantly higher (approximately 100 times higher) compared to the model based on the RootMUSIC algorithm, which is the result of avoiding complex matrix calculations.

Acknowledgment

The Ministry of Education, Science and Technological Development of the Republic of Serbia supported this work, Grants: III-44009 and TR-32052.

References

[1] GODARA, L. C. Application of antenna arrays to mobile communications, part II: Beamforming and direction-of-arrival considerations. *Proceedings of the IEEE*, 1997, vol. 85, no. 8, p. 1195–1245. DOI: 10.1109/5.622504

[2] ZOUBIR, M. A., CHELLAPPA, R., THEODORIDIS, S. *Array and Statistical Signal Processing*. Academic Press, 2014. ISBN: 978-0-12-411597-2

[3] RAO, B. D., HARI, K. V. S. Performance analysis of root-MUSIC. *IEEE Transactions on Acoustics, Speech and Signal Processing*, 1989, vol. 37, no. 12, p. 1939–1949. DOI: 10.1109/29.45540

[4] NI, Z., LUO, Y., MOTANI, M., et. al. DoA estimation for lens antenna array via Root-MUSIC, outlier detection, and clustering. *IEEE Access*, 2020, vol. 8, p. 199187–199196. DOI: 10.1109/ACCESS.2020.3034080

[5] HAYKIN, S. *Neural Networks: Comprehensive Foundation.* New York (USA): Macmillan, 1994. ISBN: 978-0023527616

[6] CHRISTODOULOU, C. G., GEORGIOPOULOS, M. *Application of Neural Networks in Electromagnetics*. Boston (USA): Artech House, 2001. ISBN: 978-0890068809

[7] ZHANG, Q. J., GUPTA, K. C. *Neural Networks for RF and Microwave Design*. Boston (USA): Artech House, 2000. ISBN: 978-1580531009

[8] CONG, J., WANG, X., HUANG, M., et. al. Robust DOA estimation method for MIMO radar via deep neural networks. *IEEE Sensors Journal*, 2021, vol. 21, no. 6, p. 7498–7507. DOI: 10.1109/JSEN.2020.3046291

[9] XIANG, H., CHEN, B., YANG, T., et. al. Improved de-multipath neural network models with self-paced feature-to-feature learning for DOA estimation in multipath environment. *IEEE Transactions on Vehicular Technology*, 2020, vol. 69, no. 5, p. 5068–5078. DOI: 10.1109/TVT.2020.2977894

[10] AGATONOVIĆ, M., STANKOVIĆ, Z., DONČOV, N., et al. Application of artificial neural networks for efficient high-resolution 2D DOA estimation. *Radioengineering*, 2012, vol. 21, no. 4, p. 1178–1186. ISSN: 1805-9600

[11] STANKOVIĆ, Z, DONČOV, N, MILOVANOVIĆ, I., et. al. Direction of arrival estimation of mobile stochastic electromagnetic sources with variable radiation powers using hierarchical neural model. *International Journal of RF and Microwave Computer-Aided Engineering*, 2019, vol. 29, no. 10, p. 1–17. DOI: 10.1002/mmce.21901

[12] BARTHELME, A., UTSCHICK, W. DoA estimation using neural network-based covariance matrix reconstruction. *IEEE Signal Processing Letters*, 2021, vol. 28, p. 783–787. DOI: 10.1109/LSP.2021.3072564

[13] LI, Y., HUANG, Y., REN, J., et. al. Robust DOA estimation in satellite systems in presence of coherent signals subject to low SNR. *IEEE Access*, 2022, vol. 10, p. 109983–109993. DOI: 10.1109/ACCESS.2022.3213712

[14] PAPAGEORGIOU, G. K., SELLATHURAI, M., ELDAR, Y. C. Deep networks for direction-of-arrival estimation in low SNR. *IEEE Transactions on Signal Processing*, 2021, vol. 69, p. 3714 to 3729. DOI: 10.1109/TSP.2021.3089927

[15] GUO, B., ZHEN, J. Coherent signal direction finding with sensor array based on back propagation neural network. *IEEE Access*, 2019, vol. 7, p. 172709–172717. DOI: 10.1109/ACCESS.2019.2956555

[16] KÜÇÜK, A., GANGULY, A., HAO, Y., et. al. Real-time convolutional neural network-based speech source localization on smartphone. *IEEE Access*, 2019, vol. 7, p. 169969–169978. DOI: 10.1109/ACCESS.2019.2955049

[17] STOICA, P., NEHORAI, A. MUSIC, maximum likelihood, and Cramer-Rao bound. *IEEE Transactions on Acoustics, Speech, and Signal Processing*, 1989, vol. 37, no. 5, p. 720–741. DOI: 10.1109/29.17564

[18] HUANG, J., WAN, Q. CRLB for DOA estimation in Gaussian and non-Gaussian mixed environments. *Wireless Personal Communication*, 2013, vol. 68, p. 1673–1688. DOI: 10.1007/s11277-012-0544-3

[19] CHEN, M., MAO, X., WANG, X. Performance analysis of deep neural networks for direction of arrival estimation of multiple sources. *IET Signal Processing*, 2023, p. 1–18. DOI: 10.1049/sil2.12178

About the Authors …

Milan ILIĆ received the Dipl.-Ing., and M.Sc. degrees in Electronic Engineering from the Faculty of Electronic Engineering, University of Nis, Serbia in 2018 and 2020 respectively. His Master's thesis was devoted to neural network modeling. He also received Dipl. Ing. degree in Information and Communication Engineering from the University of Klagenfurt, Austria in 2023. Currently, he is a research engineer at Lakeside Labs GmbH research organization with a focus on self-organizing networked systems. His interests include wireless communication technologies with a focus on embedded systems, firmware development, and the application of artificial neural networks in communication systems.

Zoran STANKOVIĆ received the Dipl.-Ing., M.Sc., and Ph.D. degrees from the Faculty of Electronic Engineering, University of Niš, Serbia, in 1994, 2002, and 2007, respectively. Currently, he is an Associate Professor at the Department of Telecommunications, Faculty of Electronic Engineering, University of Niš, Serbia. His research interests include neural network applications in the field of electromagnetics, antennas, propagation, and wireless communications systems. He is the Organizing Committee Chairman of the TELSIKS conferences since 2015. He was the recipient of the National MTT Society award in 2005 for outstanding scientific results in the area of microwave techniques.

Nataša MALEŠ-ILIĆ received the Dipl. Ing. and M.Sc. degrees in Electronic Engineering from the University of Nis, Nis, Serbia in 1992 and 1997, respectively, and the Ph.D. degree at the Department of Electronic Systems, University of Westminster, London, U.K. in 2004. She is presently a Full Professor at the Department of Telecommunications, Faculty of Electronic Engineering, Serbia. The professional orientation of Dr. Males-Ilic is toward microwave techniques and electronic, wireless communication technologies, and artificial neural network applications. Dr. Males-Ilic is the Editor in Chief of the national journal Microwave Review. She is an IEEE member, as well as a member of the IEEE Women in Engineering, the IEEE MTT-S Chapter of Serbia and Montenegro, and DAAD Alumni.